Micro-cutting tests: a new way to measure the fracture toughness and yield stress of polymeric nanocomposites

Hongjian Wang[1], Li Chang[1*], Lin Ye[1], and Gordon. J. Williams[1, 2]

[1]Aero, Mechanical and Mechatronics Engineering Department, University of Sydney, Sydney, Australia
[2]Mechanical Engineering Department, Imperial College London, South Kensington Campus, London, UK
* Corresponding author: li.chang@sydney.edu.au

Abstract

The fracture toughness, G_c, of pure epoxy and epoxy nanocomposites with 10 wt% nano-rubber and 10 wt% nano-silica particles, was determined using an orthogonal cutting method on a CNC machine. The cutting forces were measured by a multi-axis dynamometer, and depths of cut were precisely controlled from 30 μm to 120 μm. High speed cutting tools with three rake angles of 10º, 20º, and 30º were used for the cutting. The fracture results of pure epoxy and 10 wt% nano-silica epoxy composite determined by the cutting test has the same order of magnitude as which determined by the standard compact tension test. However, for 10 wt% nano-rubber epoxy, a much lower G_c value was measured due to the interaction between the plastic zone size of the crack tip and the magnitude of cutting depth. The results have indicated that orthogonal cutting could be an alternative approach to traditional LEFM testing for brittle polymeric nanocomposites. The specimen preparation and testing procedures would be greatly simplified compared with current fracture test technologies.

Keywords: Orthogonal cutting, fracture toughness, polymer nanocomposites

1. Introduction

The accurate estimation of fracture toughness for ductile, yet tough polymers remains to be a challenging task in material science. Traditional LEFM testing is affected by the blunting of the crack tip during crack propagation, which results in over-estimation of the toughness results. Recent research carried out by Patel et al. [9, 10] has proposed that orthogonal cutting may be a suitable method for measuring the strain energy release rate, G_c, for such polymers. The theory was initiated by Atkins [1-3, 5] who pointed out that the fracture energy in the orthogonal cutting process should be equally important as the plastic work and frictional loss, and that the critical fracture energy during cutting be equivalent to the cutting energy extrapolated to the zero depth of cut. Subsequently, Williams [9] developed a more sophisticated orthogonal cutting model by taking Tresca yield criterion and Coulomb friction of the workpiece material into account. A linear relationship between the cutting energy and the cutting depth with the inclusion of the constant global fracture energy, G_c, has been deduced. The new theory has been verified by the testing of some typical high toughness but low strength engineering polymers. The cutting experiment gives valid toughness results for these materials.

It is expected that this marvel fracture testing technique will also be applicable for a variety of engineering polymers, in particular, such as tough, yet brittle polymeric composites, thin polymeric film and micro-fabricated materials. The method will greatly simplify the preparation of testing specimens and avoid the limit of size requirements in the standard fracture toughness test. Our work has been focused on employing the orthogonal cutting method to measure fracture toughness of brittle amorphous epoxy and its nano-modified composites (10 wt% nano-rubber and 10 wt% nano-silica epoxies). The cutting experiment was performed on a rigid CNC machine where the depth of cut can be precisely controlled within few hundreds of microns. At this range of cutting depth, the cut material behaved sufficient plasticity. Continuous chipping process and steady-state cutting force signals were observed. The cutting condition satisfied Williams' notion of cutting tough, yet ductile polymers. Hence, the same analytical method can be used in the cutting data analysis.

2. Analysis

2.1 Orthogonal Cutting with Consideration of Fracture Energy

A schematic representation of the orthogonal cutting model developed by Williams et al. [9] is illustrated in Fig. 1 (a), where a tool with a single cutting edge of rake angle α is driven at a constant velocity V to remove a chip of thickness h_c and width b from a testing material. The force relationship of the model may be considered by treating the chip as an isolated system. During a steady-state cutting process, the chip is hold by two equal and opposite resultant forces F and F' under equilibrium condition. F' is generated by the tool which acts on the back surface of the chip; F is due to the reaction of the testing material being cut which exerts on the base of the chip. F' may be resolved into a friction force S and its normal component N along the chip back surface. S is responsible for the work expended in fraction as the chip slides over the tool rake face. On the other hand, F may be resolved into a shear force F_s and a compressive force F_n on the base of the chip. The base of the chip can be considered as a shear plane, of a shear angle φ, where shear yielding of the testing material take places. The shear force F_s is then responsible for the work expended in plastic deformation of the testing material. [7-9]

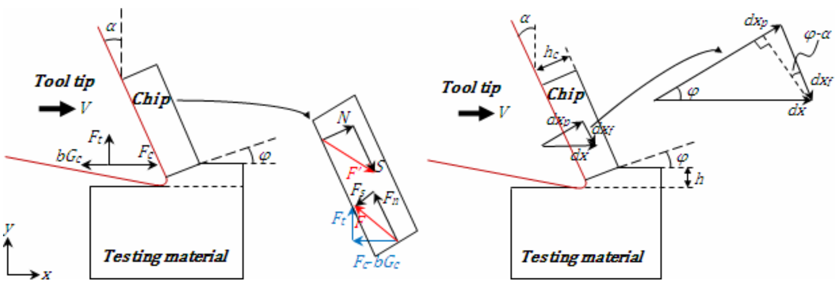

(a) (b)

Figure 1. Schematic diagrams of orthogonal cutting (a) force relationship of the cutting system and (b) geometrical relationship of displacements of forces during cutting.

From another standpoint, the resultant force, F, may also be decomposed into F_c-bG_c along the tool moving direction and F_t which is perpendicular to the tool moving direction. F_c is the cutting force delivered from the tool which is responsible for the total work dissipated in the cutting process. F_t arises from the existence of F_c, which is described as a transverse force to maintain the steady-state during cutting process. G_c is considered as the global fracture energy reserved in the testing material. Furthermore, bG_c is modelled as a reaction force towards the cutting direction to prevent the material from separation, where b represents the width of cut. [9, 10]

2.2 An Energy-based Approach to Determine the Fracture Energy

In the orthogonal cutting system as illustrated in Fig.1 (a), the total cutting energy delivered by the tool is considered to be completely dissipated into the plastic work of the chip, the frictional loss due to tool-chip interaction and the fracture work of the testing material [9], where

$$dU_{diss} = dU_{plast} + dU_{frict} + dU_{fract} \tag{1}$$

In force-displacement relation, Eq. (1) becomes

$$F_c dx = F_s dx_p + Sdx_f + bG_c dx \tag{2}$$

where dx represents the incremental displacement of tool movement. The corresponding displacements owing to F_s and S, dx_p and dx_f, respectively, can be derived based on the geometrical relationship as shown in Fig. 1 (b) [9]

$$dx_f = \frac{\sin\varphi}{\cos(\varphi-\alpha)}dx \tag{3}$$

$$dx_p = \frac{\sin\alpha}{\cos(\varphi-\alpha)}dx \tag{4}$$

Considering force equilibrium of the chip, the friction force on the tool-chip interface may be expressed as

$$S = (F_c - bG_c)\sin\alpha + F_t\cos\alpha \tag{5}$$

On the other hand, the shear force on the shear plane can be modelled in accordance with Tresca yielding criterion. It is assumed that the shear plane is formed at a critical shear stress which is half of the yield strength of the testing material [9], thus,

$$F_s = \frac{\sigma_Y}{2}\frac{bh}{\sin\varphi} \tag{6}$$

where $bh/sin\varphi$ is the effective area of the shear plane.

Substituting Eq. (3) to (6) into (2), we have

$$\frac{F_c}{b} - \frac{F_t}{b}\tan\varphi = \frac{\sigma_Y}{2}(\tan\varphi + \frac{1}{\tan\varphi})h + G_c \tag{7}$$

Thus, the fracture energy, G_c, induced by the cutting process can be determined from the linear plot of $F_c/b\text{-}(Ft/b)tan\varphi$ versus $(tan\varphi+1/tan\varphi)h$ data [9, 10], where

$$\tan\varphi = \frac{\cos\alpha}{\frac{h_c}{h} - \sin\alpha} \tag{8}$$

and h_c represents the chip thickness.

3. Experimental

3.1 Cutting Experiment Set-up

Cutting tests were carried out on a hydraulic driven rigid CNC machine (Minini Junior 90 M286). A customised tool post and a sample holder were made to cope with orthogonal cutting. The cutting forces were measured by a multi-component dynamometer (Kistler 9257B). The cutting force signals were recorded by an digital oscilloscope (Agilent 54621A) and the data were processed in Excel. A set of high speed cutting tools (Cobalt M42), of rake angles 10º, 20º and 30º and clearance angle 4º, were used in the experiment. The tools were sharpened with tip radii less than 5μm.

3.2 Testing Materials

A diglycidyl ether of bisphenol A (DGEBA) epoxy resin, Araldite-F (Ciba-Geigy, Australia), cured using piperidine (Sigma-Aldrich, Australia) with a ratio of 100:5 (epoxy/piperidine), was used as the base material. For two epoxy nanocomposites, one has 10 wt% SiO_2 nanoparticle produced from Nanopox XP 22/0616 resin (Hanse-Chemie AG, Germany), which consists of well dispersed silica nanoparticles (40 wt%) with an average particle size of 20 nm, while the other has 10 wt% spherical rubber particle produced from a bisphenol master batch resin with 25 wt% well dispersed rubber nanoparticles of 100 nm in size (Kaneka Corporation, Japan). [6, 11] For the cutting experiment, the testing materials were prepared into approximately 5mm thick rectangular blocks.

The values of fracture toughness G_c and yielding stress σ_Y of the testing materials have been determined from conventional compact tension and tensile tests [6, 11], where the CT test followed ASTM D5045 while the tensile test followed ASTM D638.

3.3 Cutting Test Method

The testing material and tool were firmly gripped on the sample holder and tool post, respectively. Cutting started with first a few thin sectioning of the testing material in order to flatten the cut surface. Subsequently, consecutive cutting operation was performed with a speed of *1 mm/s* and the depths of cut were varied from 30μm to 120μm. After each cut, the chip was collected for further measurement.

4. Results and Discussion

4.1 Cutting Results for Pure Epoxy and Epoxy Nanocomposites

Cutting results are presented for pure epoxy and two epoxy nanocomposites. Cutting forces F_c and F_t, and chip thickness h_c are measured for a range of cutting depths h. The data are evaluated by Eq. 7, as shown in Fig. 2.

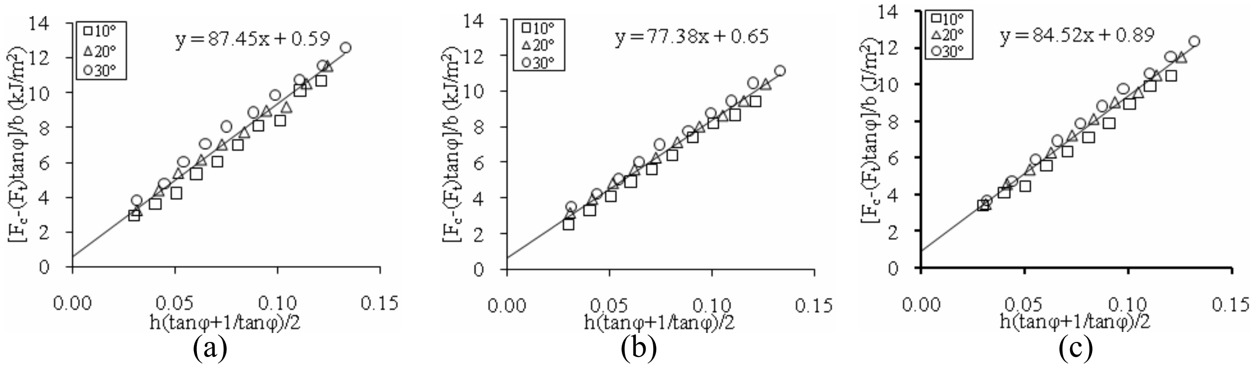

Figure 2. Cutting results for (a) pure epoxy with specimen width b=5.57*mm*, (b) 10% nano-rubber epoxy with specimen width b=5.04*mm*, and (c) 10% nano-silica epoxy with specimen width b=5.40*mm*. The cutting velocity was at *1 mm/s*. The legend shows the rake angle in degrees.

Table 1. Yield stress and fracture toughness for epoxy and its nanocomposites [6, 11].

		Pure epoxy		10% nano-rubber epoxy		10% nano-silica epoxy	
Method	Testing rate	$\sigma_Y\,(MPa)$	$G_c\,(kJ/m^2)$	$\sigma_Y\,(MPa)$	$G_c\,(kJ/m^2)$	$\sigma_Y\,(MPa)$	$G_c\,(kJ/m^2)$
Cutting test	1mm/s	87.46±2.47	0.59±0.21	77.38±1.25	0.65±0.09	84.52±1.73	0.89±0.15
CT test	1mm/min	--	0.28±0.25	--	1.93±0.1	--	0.69±0.05

Tensile test	5mm/min	42.1±2.6	--	37.6±0.8	--	46.5±1.1	--

The linear regression analysis has been shown in the plots of $F_c/b-(F_t/b)tan\varphi$ versus $(tan\varphi+1/tan\varphi)h$ data. The gradient gives the yield stress, σ_Y, which was deduced in accordance with Tresca yield criterion, and the y-intercept is the fracture energy, G_c, of the testing material induced by cutting. The σ_Y and G_c determined from the cutting test are compared with those determined from standard compact tension and uni-axial tensile tests, as listed in Tab. 1.

4.2 Results Discussion

The compact tension test gives G_c values of 0.28±0.25 kJ/m^2, 1.93±0.1 kJ/m^2 and 0.69±0.05 kJ/m^2 for pure epoxy, 10% nano-rubber epoxy and 10% nano-silica epoxy, respectively. Cutting test gives higher G_c results for pure epoxy and 10% nano-silica epoxy, but within reasonable limits. The cause of discrepancy is attributed to the complication in the estimation of depth of cut, h. Since the tool cannot be perfectly sharp, the lower portion of the tool tip may result in a ploughing of the testing material during the cutting process. Thus, the measurements of the cutting depth were overestimated by the size of δ, as shown in Fig. 3 (b).

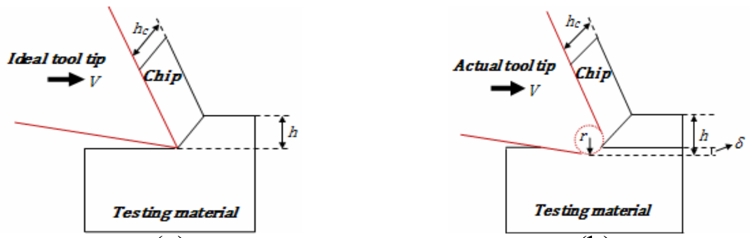

(a) (b)

Figure 3. Schematics of orthogonal cutting with (a) an ideal sharp tool, and (b) an actual tool with a tip radius *r*.

Assuming that half size of the tip radius contributes to the ploughing process, the fracture energy that was over estimated by ploughing could be approximated by

$$G' = \delta\sigma_Y \tag{9}$$

where the tool tip radius used in the experiment was around 5μm; σ_Y is the yield stress determined from the cutting test. [4] Hence, the actual fracture energy induced by cutting for pure epoxy becomes

$$G_c = 0.59kJ/m^2 - \frac{2.5\times 87.46}{1000}kJ/m^2 \approx 0.37kJ/m^2 \tag{10}$$

and also, for 10% nano-silica epoxy

$$G_c = 0.89kJ/m^2 - \frac{2.5\times 84.52}{1000}kJ/m^2 \approx 0.68kJ/m^2 \tag{11}$$

which are in good agreement with the results derived from the compact tension test.

The cutting test gives 0.65±0.09 kJ/m^2 for the G_c value of 10% nano-rubber epoxy. The result is about 3 times lower than that given by the compact tension test. In this particular case, the cutting result is most likely affected by the crack tip plastic zone size of the testing material. The estimated plastic zone size in the compact tension test for 10% nano-rubber epoxy is about 190μm, which is far above the nominal depth of cut for the cutting test: 30μm to 120μm. Thus, the plastic zone size induced by cutting is confined and the measured G_c value is much more conservative.

Finally, it is noticed that cutting method always determines high values of yield stress compared with those determined from the tensile test. This has been ascribed to large strain and high strain rate on the shear plane during the chip formation process [9].

5. Conclusion

The fracture toughness of epoxy and its epoxy nanocomposites with 10 wt% rubber and silica nanoparticle has been measured by use of an orthogonal cutting method. The cutting method has been proven as a valid way to characterise the G_c of ductile and moderately tough polymeric materials [10]. This work expands the applicability of the method to brittle and tough amorphous polymer and its nanocomposites. It is believed that with the careful examination of the cutting quantities and the material property, orthogonal cutting could become an alternative approach to easily determine the fracture toughness of a wide variety of engineering polymers.

Reference

[1] Atkins AG. Modelling metal cutting using modern ductile fracture mechanics: quantitative explanations for some longstanding problems. International Journal of Mechanical Sciences. 2003;45(2):373-396.

[2] Atkins AG. Toughness and cutting: a new way of simultaneously determining ductile fracture toughness and strength. Eng Fract Mech. 2005;72(6):849-860.

[3] Atkins AG, Vincent JFV. An Instrumented Microtome for Improved Histological Sections and the Measurement of fracture Toughness. J Mater Sci Lett. 1984;3(4):310-312.

[4] Blackman BRK, Hoult TR, Patel Y, Williams JG. Tool sharpness as a factor in machining tests to determine toughness. Eng Fract Mech;101(0):47-58.

[5] Ericson ML, Lindberg H. Design and potential of instrumented ultramicrotomy. Polymer. 1997;38(17):4485-4489.

[6] Liu HY, Wang GT, Mai YW, Zeng Y. On fracture toughness of nano-particle modified epoxy. Compos Pt B-Eng. 2011;42(8):2170-2175.

[7] Merchant E. MECHANICS OF THE METAL CUTTING PROCESS .1. ORTHOGONAL CUTTING AND A TYPE-2 CHIP. J Appl Phys. 1945;16(5):267-275.

[8] Merchant ME. MECHANICS OF THE METAL CUTTING PROCESS .2. PLASTICITY CONDITIONS IN ORTHOGONAL CUTTING. J Appl Phys. 1945;16(6):318-324.

[9] Patel Y, Blackman BRK, Williams JG. Determining fracture toughness from cutting tests on polymers. Eng Fract Mech. 2009;76(18):2711-2730.

[10] Patel Y, Blackman BRK, Williams JG. Measuring fracture toughness from machining tests. Proc Inst Mech Eng Part C-J Eng Mech Eng Sci. 2009;223(12):2861-2869.

[11] Zhang J, Deng S, Ye L. Roles of rigid nano-particles and CTBN rubber in toughening DGEBA epoxies with different cross-linking densities. ACUN 6. Melbourne; 2012.